Environ. Sci. Technol. **2004**, *38*, 5567−5576

Study of the OH and Cl-Initiated Oxidation, IR Absorption Cross-Section, Radiative Forcing, and Global Warming Potential of Four C_4-Hydrofluoroethers

NATHAN OYARO,
STIG R. SELLEVÅG, AND
CLAUS J. NIELSEN*

Department of Chemistry, University of Oslo, P. O. Box 1033, Blindern, N-0315 Oslo, Norway

Infrared absorption cross-sections and OH and Cl reaction rate coefficients for four C_4-hydrofluoroethers $(CF_3)_2CHOCH_3$, $CF_3CH_2OCH_2CF_3$, $CF_3CF_2CH_2OCH_3$, and $CHF_2CF_2CH_2OCH_3$ are reported. Relative rate measurements at 298 K and 1013 hPa of OH and Cl reaction rate coefficients give $k(OH+(CF_3)_2CHOCH_3) = (1.27 \pm 0.13) \times 10^{-13}$, $k(OH+CF_3CH_2OCH_2CF_3) = (1.51 \pm 0.24) \times 10^{-13}$, $k(OH+CF_3CF_2CH_2OCH_3) = (6.42 \pm 0.33) \times 10^{-13}$, $k(OH+CHF_2CF_2CH_2OCH_3) = (8.7 \pm 0.5) \times 10^{-13}$, $k(Cl+(CF_3)_2CHOCH_3) = (8.4 \pm 1.3) \times 10^{-12}$, $k(Cl+CF_3CH_2OCH_2CF_3) = (6.5 \pm 1.7) \times 10^{-13}$, $k(Cl+CF_3CF_2CH_2OCH_3) = (4.0 \pm 0.8) \times 10^{-11}$, and $k(Cl+CHF_2CF_2CH_2OCH_3) = (2.65 \pm 0.17) \times 10^{-11}$ cm^3 molecule^{-1} s^{-1}. The primary products of the OH and Cl reactions with the fluorinated ethers have been identified as esters, and OH and Cl reaction rate coefficients for one of these, CF_3CH_2OCHO, are reported: $k(OH+CF_3CH_2OCHO) = (7.7 \pm 0.9) \times 10^{-14}$ and $k(Cl+CF_3CH_2OCHO) = (6.3 \pm 1.9) \times 10^{-14}$ cm^3 molecule^{-1} s^{-1}. The rate coefficient for the Cl-atom reaction with CHF_2CH_2F is derived as $k(Cl+CHF_2CH_2F) = (3.0 \pm 0.9) \times 10^{-14}$ cm^3 molecule^{-1} s^{-1} at 298 K. The error limits include 3σ from the statistical data analyses as well as the errors in the rate coefficients of the reference compounds employed. The tropospheric lifetimes of the hydrofluoroethers are estimated to be short $\tau_{OH}((CF_3)_2CHOCH_3) \sim 100$ days, $\tau_{OH}(CF_3CH_2OCH_2CF_3) \sim 80$ days, $\tau_{OH}(CF_3CF_2CH_2OCH_3) \sim 20$ days, and $\tau_{OH}(CHF_2CF_2CH_2OCH_3) \sim 14$ days, and their global warming potentials are small compared to CFC-11.

Introduction

The identification of suitable industrial alternatives to CFCs and HCFCs remains a challenge due to the complex combination of performance, safety, and environmental properties required. Hydrofluoroethers, HFEs, have been suggested as replacement compounds for CFCs and HFCs in applications such as the cleaning of electronic components, refrigeration, and carrier compounds for lubricants. Removal of HFEs from the troposphere will essentially be initiated by reaction with OH radicals although the reactions with Cl atoms may be of some importance in the marine boundary layer. To ascertain the environmental impact of HFEs released into the troposphere, their atmospheric lifetimes with respect to reaction with OH radicals and the nature and fate of the resulting oxidation products are required.

As part of the ongoing work in our laboratory concerning the atmospheric chemistry of fluorinated alcohols and ethers we have studied the reactions of OH radicals and Cl atoms with bis(trifluoromethyl)methyl methyl ether ($(CF_3)_2CHOCH_3$, 356mmzE$\beta\gamma$, Iso-flurothyl, Isoindoklon), bis(2,2,2-trifluoroethyl) ether ($CF_3CH_2OCH_2CF_3$, Fluorothyl, Fluroethyl, Flurothyl, Flurotyl, HFE-356mf-f, Idoklon, Indiklon, Indoklon, SKF 6539), 2,2,3,3-tetrafluoropropyl methyl ether ($CHF_2CF_2CH_2OCH_3$, HFE-374pcf), and 2,2,3,3,3-pentafluoropropyl methyl ether ($CF_3CF_2CH_2OCH_3$, HFE-365mcf, 365sfE$\gamma\delta$).

There are no relevant experimental data available for $(CF_3)_2CHOCH_3$, $CHF_2CF_2CH_2OCH_3$, and $CF_3CF_2CH_2OCH_3$. For $CF_3CH_2OCH_2CF_3$ the kinetics of the OH reaction was studied by the flash photolysis resonance fluorescence technique over the temperature range 277−370 K (*1*) and by the relative rate technique using GC detection (*2*), while the Cl atom reaction was studied in a VLPR flow system in the temperature range 273−363 K (*3*) and by the relative rate technique at room temperature using FTIR detection (*4*). Two studies report the products formed in the Cl atom initiated oxidation of $CF_3CH_2OCH_2CF_3$ (*2*, *4*), and the IR absorption cross sections for $CF_3CH_2OCH_2CF_3$ have been presented by Orkin et al. (*1*) and Sihra et al. (*5*) along with estimates of its radiative forcing and global warming potential.

Experimental Section

IR and UV−vis Absorption Cross-Sections. The absorption cross-section of a compound J at a specific wavenumber $\tilde{\nu}$ is according to Beer−Lambert's law given by $\sigma(\tilde{\nu}) = A_e(\tilde{\nu})/n_J l$, where $A_e(\tilde{\nu}) = -\ln \tau(\tilde{\nu})$ is the naperian absorbance, τ is the transmittance, n_J is the number density of J, and l is the path length where the absorption takes place. The integrated absorption cross-section, S_{int}, is given by

$$S_{int} = \int_{band} \sigma(\tilde{\nu}) d\tilde{\nu} \quad (1)$$

Absolute integrated absorption cross-sections of $(CF_3)_2CHOCH_3$, $CF_3CH_2OCH_2CF_3$, $CF_3CF_2CH_2OCH_3$, and $CHF_2CF_2CH_2OCH_3$ were measured at 298(2) K in the region 4000−400 cm^{-1}. Fourier transform infrared (FTIR) spectra of the pure vapors were recorded using a Bruker IFS 113v spectrometer employing a nominal resolution of 1.0 cm^{-1} and Blackman-Harris 3-Term apodization of the interferograms. A Ge/KBr beam splitter was used to cover the spectral region. To ensure optical linearity, a deuterated triglycine sulfate (DTGS) detector was used. Eight single channel spectra each recorded with 32 scans were averaged to yield one background or sample spectrum. Background spectra of the empty cell were recorded before and after each sample spectrum. An average of the two transmittance spectra was used in the succeeding analysis. A gas cell of 2.34(2) cm length equipped with KBr windows was employed. Three independent experiments were performed. The partial pressures of the gases were in the range between 1.8 and 8 hPa and were measured using an absolute pressure transducer (MKS Baratron Type 122A) with a stated accuracy of ±0.15%.

Absorption cross-sections in the UV−vis region were measured at 298(2) K using an Agilent 8453E photodiode array spectrophotometer having a spectral resolution of 2 nm. The spectra were recorded in the wavelength range from 190 to 1100 nm at sampling intervals of 1 nm. The integration time was set to 0.5 s. The pressures of the pure vapors were in the range 3 to 95 hPa and were measured using a MKS

* Corresponding author phone: +47 22855680; fax: +47 22855441; e-mail: claus.nielsen@kjemi.uio.no.

10.1021/es0497330 CCC: $27.50
Published on Web 09/22/2004

Baratron Type 122A pressure transducer. A gas cell of 8.0(1) cm length with quartz windows was used.

Relative Rate Measurements. The reaction rate coefficients were determined by the relative rate method

$$S + X \xrightarrow{k_S} \text{Prod}$$

$$R + X \xrightarrow{k_R} \text{Prod} \qquad (2)$$

where S is the substrate of interest, R is the reference compound, X is the radical, and k_S and k_R are the reaction rate coefficients. Assuming that the substrate and reference compounds are lost solely via reaction with the radical species of interest and that they are not reformed in any process, the relative rate coefficient, k_{rel}, can be obtained by the following relation

$$\ln\left\{\frac{[S]_0}{[S]_t}\right\} = k_{rel}\cdot\ln\left\{\frac{[R]_0}{[R]_t}\right\}; \quad k_{rel} = \frac{k_S}{k_R} \qquad (3)$$

in which $[S]_0$, $[R]_0$, $[S]_t$, and $[R]_t$ denote the concentrations of S and R at time zero and t, respectively. A plot of $\ln\{[S]_0/[S]_t\}$ vs $\ln\{[R]_0/[R]_t\}$ will give k_{rel} as the slope. Data from independent experiments were analyzed jointly according to eq 3 using a weighted least squares procedure including uncertainties in both reactant concentrations (*6*); the uncertainties in the reactant concentrations were taken as the variance in three consecutive measurements but not less than 1%. The quoted errors in this work represent the 3σ statistical errors and include the uncertainty in the reference reaction rate coefficients, but not any possible systematic errors.

The measurements were performed at 1013 ± 15 hPa and 298 ± 2 K in synthetic air in a 250 L smog chamber of electropolished stainless steel. In situ air analyses were obtained with an Agilent 6890/5973 GC-MS employing chemical ionization (CI). The GC was operated under isothermal conditions at 40 °C. A constant overpressure of ca. 5 hPa was applied to the reactor to ensure a steady flow of ca. 20 mL/min through a 0.5 mL GC sampling loop the content of which was injected into the GC in a 1:50 split mode using helium as the carrier gas. The column used for the separation was DB-Waxetr with a length of 30 m, internal diameter of 0.25 mm, and film coating of 0.25 μm. The DB-Waxetr column was coated with a poly(ethylene glycol). The inlet and the sample loop temperatures were kept constant at 100 °C.

An inert tracer (1,2-perfluorodimethylcyclohexane) was added in initial experiments to monitor the dilution of the reactants due to the constant flow out of the reactor—the dilution was in all cases negligible. The positive chemical ionization (PCI) mode employing CH_5^+ was used, as it is a soft method of ionization with little fragmentation of the reactants and the products. As a first step, the full scan mode was selected to obtain complete mass spectra to identify the reactants and the reaction products in the gas-chromatograms. The compounds studied, the reference compounds, and the reaction products all had unique mass peaks, which made it possible to operate the MS in the Selective Ion Mode, SIM, in which only chosen m/z numbers are followed. The SIM mode was then employed for the quantification of the individual compounds, the advantage being a reduced background noise and the elimination of overlap in cases of incomplete gas-chromatographic separation.

The relative concentrations of the HFEs $(CF_3)_2CHOCH_3$, $CF_3CH_2OCH_2CF_3$, $CHF_2CF_2CH_2OCH_3$, and $CF_3CF_2CH_2OCH_3$, and the ester CF_3CH_2OCHO were determined from the m/z signals at 183 $[(CF_3)_2CHOCH_3]H^+$, 183 $[CF_3CH_2OCH_2CF_3]H^+$, 147 $[CH_3OCH_2CF_2CHF_2]H^+$, 165 $[CF_3CF_2CH_2OCH_3]H^+$, and 129 $[CF_3CH_2OCHO]H^+$, respectively, and/or from the daughter ions with $m/z = M-19$ resulting from HF elimination from the MH^+-ions. The relative concentrations of the reference compounds CH_3OH, CH_3CH_2OH, CH_2Cl_2, $CHCl_3$, CH_2ClCH_2Cl, CH_2FCHF_2, $CF_3CH_2OCH_3$, and $C_4F_9OC_2H_5$ were determined from the m/z signals at 33 $[CH_3OH]H^+$, 47 $[CH_3CH_2OH]H^+$, 49 ($[CH_2Cl_2]H^+ - HCl$), 83 ($[CHCl_3]H^+ - HCl$), 63 ($[CH_2ClCH_2Cl]H^+ - HCl$), 65 ($[CH_2FCHF_2]H^+ - HF$), 115 $[CF_3CH_2OCH_3]H^+$, and 245 ($[C_4F_9C_2H_5]H^+ - HF$). The PCI-MS spectra of all compounds used are given as Supporting Information.

Chemicals. Hydroxyl radicals were generated by photolysis of O_3 in the presence of H_2 employing a Philips TUV 30W lamp ($\lambda_{max} \sim 254$ nm) mounted in a quartz tube in the smog chamber. The lamp was turned off during recording of the spectra.

$$O_3 + h\nu\ (\lambda_{max} \sim 254\ \text{nm}) \rightarrow O(^1D) + O_2 \qquad (4)$$

$$O(^1D) + H_2 \rightarrow OH + H \qquad (5)$$

This OH production scheme produces not only OH radicals in the ground-state but also in excited vibrational states (*7*–*9*). However, the collisional quenching rate coefficient of OH by O_2 and N_2 is of the order of 10^{-10} cm^3 molecule^{-1} s^{-1} (*10*), that is 2 to 3 orders of magnitude faster than the OH reaction rate coefficients of the HFEs and the reference compounds. In addition, the mixing ratios of O_2 and N_2 are 5 orders of magnitude larger than those of the HFEs and the reference compounds, and one may therefore safely assume that the HFEs and the reference compounds react exclusively with OH in the vibrational ground state.

Ozone was produced from oxygen by using a TRI-OX Ozone Generator model T-200 that converts approximately 2% of the oxygen gas flow to ozone. Cl atoms were generated by photolysis of Cl_2 using two Philips TL 18W/08 fluorescence lamps ($\lambda_{max} \sim 375$ nm); photolysis was carried out in time intervals of 1 to 20 min. Typical mixing ratios were as follows: HFEs and reference compounds, 2–6 ppm; Cl_2, 5–10 ppm; H_2, 1000 ppm; O_3, 100–400 ppm. Synthetic air (CO + NOx < 100 ppb, C_nH_m < 1 ppm), helium (99.9999%), hydrogen (99%), and oxygen gas (99.95%) were delivered from AGA. CF_3CH_2OCHO was synthesized from CF_3CH_2OH (Fluorochem Ltd.) and concentrated HCOOH and purified by standard methods. $(CF_3)_2CHOCH_3$ (purity 97%), $CHF_2CF_2CH_2OCH_3$ (purity 97%), and $CF_3CF_2CH_2OCH_3$ (purity 97%) originated from Fluorochem Ltd., $CF_3CH_2OCH_2CF_3$ (purity 99%) from Aldrich, and $C_4F_9OC_2H_5$ from 3M, while the other reference compounds were standard laboratory chemicals. The samples were distilled in a vacuum prior to use. The only impurity observed in the gaseous HFEs by IR and headspace GC-MS was CF_2O, which was removed by single-plate vacuum distillation at −78 °C.

Results and Discussion

IR Absorption Cross-Sections. Infrared absorption cross-sections were determined from the absorbance spectra assuming that the gas was ideal and applying a baseline correction. The latter was performed by subtracting a polynomial function, obtained by fitting the regions of the spectrum where no absorptions were expected. The integrations over the absorption bands were carried out using a method that defines the baseline from an average of two points on one side of the band and the average of two points on the other side of the band.

The integrated absorption cross-section of the absorption bands, or regions of overlapping bands, was determined by plotting the integrated absorbance against the product of the number density and the path length. Since none of the regression lines had a y-intercept significantly different from

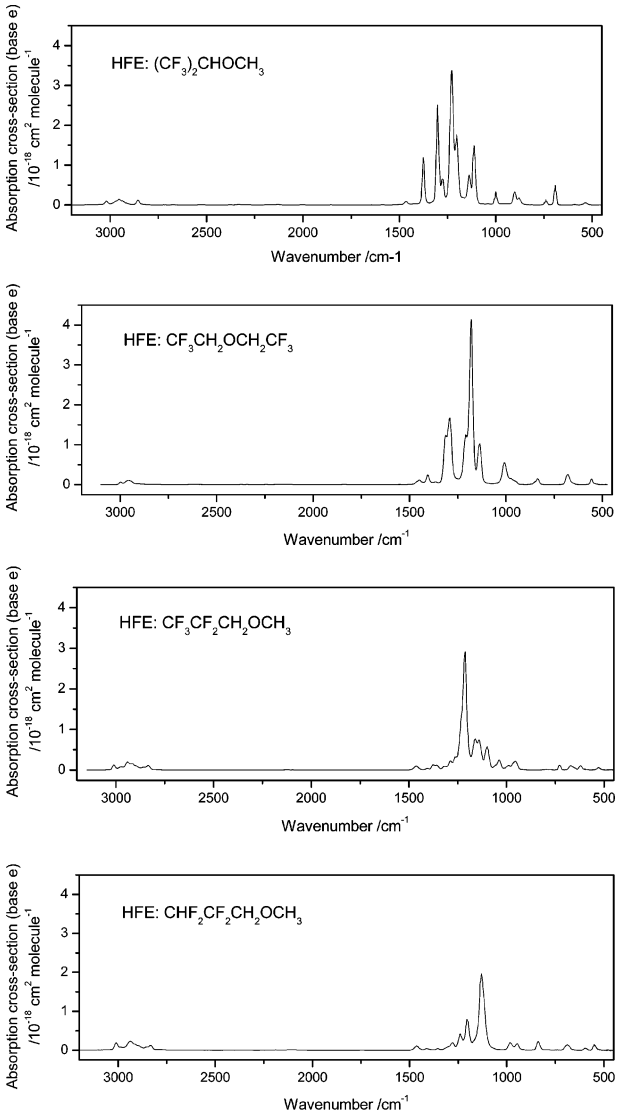

FIGURE 1. Infrared absorption cross-sections (base e) of four C_4-HFEs: $(CF_3)_2CHOCH_3$, $CF_3CH_2OCH_2CF_3$, $CF_3CF_2CH_2OCH_3$, and CHF_2CF_2-CH_2OCH_3.

TABLE 1. Absolute Absorption Cross-Sections, S_{int}, of Four C_4-Hydrofluoroethers in the Mid-Infrared Region

compound	spectral region/cm^{-1}	S_{int}/10^{-17} cm molecule^{-1}	reference
$(CF_3)_2CHOCH_3$	1550−475	25.8 ± 0.4	this work
$CF_3CH_2OCH_2CF_3$	1600−500	27.2 ± 1.0	this work
	1600−500	27.7 ± 0.3	Orkin et al. (*1*)
	2000−450	27.33	Sihra et al. (*5*)
$CF_3CF_2CH_2OCH_3$	1525−490	19.46 ± 0.24	this work
$CHF_2CF_2CH_2OCH_3$	1520−500	13.91 ± 0.23	this work

zero, a least-squares method that forced the regression line through zero was used to determine the absorption cross-sections. Uncertainties in pressure measurements (0.15%), path length (0.90%), and temperature (0.67%) have been quantified as systematic errors. The uncertainty in path length includes both geometrical and optical errors.

The absorption cross-sections (base e) of $(CF_3)_2CHOCH_3$, $CF_3CH_2OCH_2CF_3$, $CF_3CF_2CH_2OCH_3$, and $CHF_2CF_2CH_2OCH_3$ in the 3200−450 cm^{-1} region are shown in Figure 1. The integrated absorption cross-sections are summarized in Table 1. As can be seen, the estimated uncertainty in the total absorption cross-section of the HFEs is less than two percent

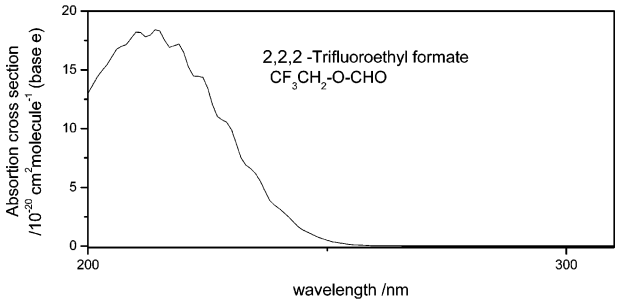

FIGURE 2. UV absorption cross-section (base e) of 2,2,2-trifluoroethyl formate.

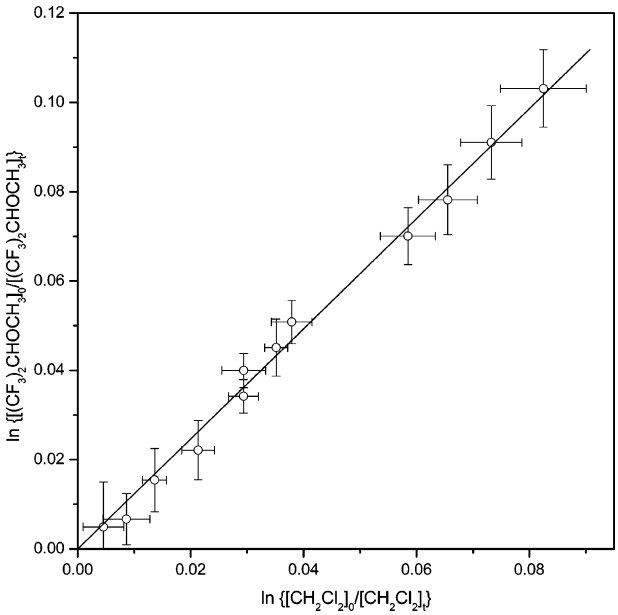

FIGURE 3. Decay of $(CF_3)_2CHOCH_3$ and CH_2Cl_2 in the presence of OH radicals at 298 K plotted as of ln{[$(CF_3)_2CHOCH_3$]$_0$/[$(CF_3)_2CHOCH_3$]$_t$} vs ln{[CH_2Cl_2]$_0$/[CH_2Cl_2]$_t$}. Twelve data points from 2 independent experiments were analyzed according to eq 2 giving a relative rate k_{rel} = 1.24 ± 0.07 (3σ error).

and includes error from the least-squares fit and the above-mentioned systematic errors.

Quantitative measurements of the infrared absorption cross-section of $CF_3CH_2OCH_2CF_3$ have previously been reported by Orkin et al. (*1*) (1600−500 cm^{-1}) and Sihra et al. (*5*) (2000−450 cm^{-1}). Their results are in perfect agreement with the present work, see Table 1. We use the absorption cross-section of HCFC-22, which has been critically evaluated by Ballard et al. (*11*), as a benchmark. Our measurements of HCFC-22 are constantly within 5% of the absorption cross-section reported by Ballard and co-workers. We therefore believe that our measurements of the HFEs are not affected by any large systematic errors.

UV Absorption Cross-Sections. The HFEs studied do not absorb radiation above 200 nm. 2,2,2-Trifluoroethyl formate, CF_3CH_2−O−CHO, is a representative example of the class of compounds (esters) formed in the atmospheric oxidation of HFEs (*2, 4*), and its UV absorption cross-section is presented in Figure 2. As can be seen, the absorption of the formate falls below 250 nm, and one may conclude that saturated fluorinated esters, like their hydrocarbon analogues, do not undergo photolysis in the troposphere.

Relative Rate Measurements. The OH reaction with $(CF_3)_2CHOCH_3$ was studied using CH_2Cl_2 and $C_4F_9OC_2H_5$ as reference compounds. Figure 3 shows a plot of ln{[$(CF_3)_2$-$CHOCH_3$]$_0$/[$(CF_3)_2CHOCH_3$]$_t$} vs ln{[CH_2Cl_2]$_0$/[CH_2Cl_2]$_t$} during the reaction with OH radicals; analysis of data from two

TABLE 2. Relative Rate Coefficients and Derived Absolute Rate Coefficients for the OH Radical Reaction with a Series of Fluorinated Ethers and Esters at 298 K

HFE	reference compound[a]	k_{rel}	k_{OH}/cm^3 molecule^{-1} s^{-1}	method[b]
$(CF_3)_2CHOCH_3$	$C_4F_9OCH_2CH_3$	1.26 ± 0.08	(1.30 ± 0.16) × 10^{-13}	RR-GC/MS
	CH_2Cl_2	1.24 ± 0.07	(1.24 ± 0.20) × 10^{-13}	RR-GC/MS
$CF_3CH_2OCH_2CF_3$	$CHCl_3$	1.51 ± 0.07	(1.51 ± 0.24) × 10^{-13}	RR-GC/MS
			(1.68 ± 0.09) × 10^{-13}	FP−RF (*1*)
			(1.01 ± 0.15) × 10^{-13}	RR-GC (*2*)
$CF_3CF_2CH_2OCH_3$	$CF_3CH_2OCH_3$	1.158 ± 0.016	(6.42 ± 0.33) × 10^{-13}	RR-GC/MS
$CHF_2CF_2CH_2OCH_3$	$CF_3CH_2OCH_3$	1.55 ± 0.06	(8.6 ± 0.5) × 10^{-13}	RR-GC/MS
	$CHCl_3$	9.8 ± 0.9	(9.8 ± 1.7) × 10^{-13}	RR-GC/MS
CF_3CH_2OCHO	$CHCl_3$	0.720 ± 0.026	(7.2 ± 1.1) × 10^{-14}	RR-GC/MS
	CH_2ClCH_2Cl	0.415 ± 0.027	(1.03 ± 0.32) × 10^{-13}	RR-GC/MS
	CHF_2CH_2F	4.8 ± 0.4	(8.2 ± 1.8) × 10^{-14}	RR-GC/MS

[a] Reaction rate coefficients of reference compounds (/cm^3 molecule^{-1} s^{-1}): $k(OH+C_4F_9OCH_2H_3)$ = (1.0 ± 0.11) × 10^{-13} (*13*), $k(OH+CH_2Cl_2)$ = (1.0 ± 0.15) × 10^{-13} (*12*), $k(OH+CHCl_3)$ = (1.0 ± 0.15) × 10^{-13} (*12*), $k(OH+CF_3CH_2OCH_3)$ = (5.54 ± 0.27) × 10^{-13} (*17*, *18*), $k(OH+CH_2ClCH_2Cl)$ = (2.5 ± 0.7) × 10^{-13} (*19*), $k(OH+CHF_2CH_2F)$ = (1.7 ± 0.34) × 10^{-14} (*12*). [b] RR, relative rate; GC, gas chromatography; MS, mass spectrometry; FP-RF, flash-photolysis resonance-fluorescence.

independent experiments according to eq 3 give $k_{rel} = k(OH+(CF_3)_2CHOCH_3)/k(OH+CH_2Cl_2)$ = 1.24 ± 0.07, where the quoted error in the relative rate coefficient represents the 3 σ statistical error. The latest JPL data evaluation (*12*) has recommended a rate coefficient of (1.0 ± 0.15) × 10^{-13} cm^3 molecule^{-1} s^{-1} for the reaction between OH and CH_2Cl_2 at 298 K. On an absolute scale, the derived OH reaction rate coefficient of $(CF_3)_2CHOCH_3$ is therefore (1.24 ± 0.20) × 10^{-13} cm^3 molecule^{-1} s^{-1}, Table 2. The experimental data from a relative rate study using $C_4F_9OC_2H_5$ (HFE7200) as the reference compound, shown in graphical form as Supporting Information, gives $k(OH+(CF_3)_2CHOCH_3)/k(OH+HFE7200)$ = 1.26 ± 0.08. Using the most recent rate coefficient for the reaction between OH and HFE7200 of (1.03 ± 0.11) × 10^{-13} cm^3 molecule^{-1} s^{-1} at 298 K (*13*) places the OH rate coefficient of $(CF_3)_2CHOCH_3$ at (1.30 ± 0.16) × 10^{-13} cm^3 molecule^{-1} s^{-1} and the weighted average of our results at (1.27 ± 0.13) × 10^{-13} cm^3 molecule^{-1} s^{-1}. The product study, see later, shows that the oxidation of $(CF_3)_2CHOCH_3$ results in generation of CF_3 and thereby in CF_3O radicals. It is known that CF_3O reacts with CH_2FCl (*14*) and CF_3CH_2F (*15*) with rate coefficients of 1.2 × 10^{-14} and 1.1 × 10^{-15} cm^3 molecule^{-1} s^{-1}, respectively, and we anticipate a rate coefficient < 1 × 10^{-13} cm^3 molecule^{-1} s^{-1} for its reaction with the substrate and reference compounds in the present experiments. A conservative estimate of the CF_3O rate coefficient for reaction with H_2, resulting in CF_3OH and H atoms, is 2 × 10^{-14} cm^3 molecule^{-1} s^{-1} (*16*). As the concentration of H_2, which was used as the OH source by reaction with O(^{1}D), is approximately 3 orders of magnitude larger than those of the substrate and reference compounds in our experiments, we conclude H_2 will act as a scavenger for CF_3O radicals in the reactor.

The OH reaction with $CF_3CH_2OCH_2CF_3$ was studied using $CHCl_3$ as reference compound giving $k(OH+CF_3CH_2OCH_2CF_3)/k(OH+CHCl_3)$ = 1.51 ± 0.07, Table 2. The experimental data are given in graphical form as Supporting Information. The latest JPL data evaluation (*12*) has recommended rate coefficients of (1.0 ± 0.15) × 10^{-13} cm^3 molecule^{-1} s^{-1} at 298 K for the OH reaction of $CHCl_3$, and we derive a value for the OH reaction rate coefficient of $CF_3CH_2OCH_2CF_3$ (1.51 ± 0.24) × 10^{-13} cm^3 molecule^{-1} s^{-1}, Table 2. The product study, see later, shows that the oxidation of $CF_3CH_2OCH_2CF_3$ results in generation of CF_3 and thereby in CF_3O radicals. As mentioned above, with its large concentration in the system H_2 will act as a scavenger for CF_3O radicals, and our results should not be influenced by reactions of this radical. The present result also compares well with the absolute reaction rate coefficient carefully determined by Orkin et al. (*1*)

The kinetics of the OH + $CF_3CF_2CH_2OCH_3$ and OH + $CHF_2CF_2CH_2OCH_3$ reactions was investigated simultaneously using

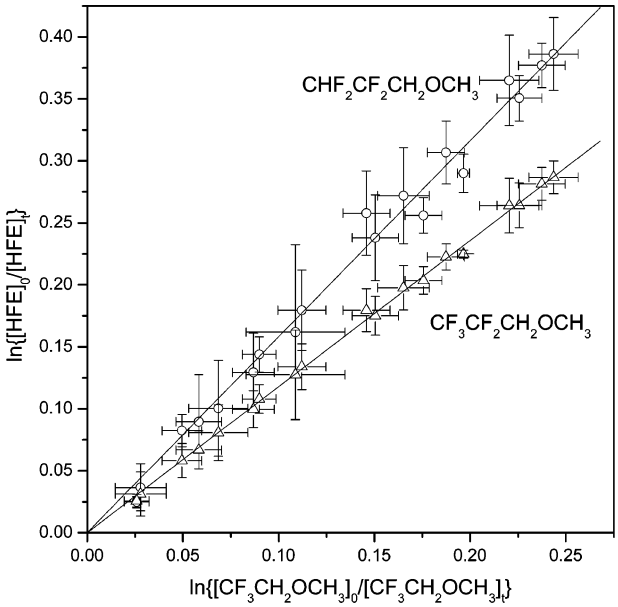

FIGURE 4. Decays of $CF_3CF_2CH_2OCH_3$ (Δ), $CHF_2CF_2CH_2OCH_3$ (○), and $CF_3CH_2OCH_3$ in the presence of OH radicals at 298 K plotted as ln{$[CF_3CF_2CH_2OCH_3]_0/[CF_3CF_2CH_2OCH_3]_t$} and ln{$[CHF_2CF_2CH_2OCH_3]_0/[CHF_2CF_2CH_2OCH_3]_t$} vs ln{$[CF_3CH_2OCH_3]_0/[CF_3CH_2OCH_3]_t$}. Nineteen data points for each compound from 2 independent experiments were analyzed according to eq 2 giving the relative rates k_{rel} = 1.158 ± 0.016 and k_{rel} = 1.55 ± 0.06 (3σ error) for $CF_3CF_2CH_2OCH_3$ and $CHF_2CF_2CH_2OCH_3$, respectively.

$CF_3CH_2OCH_3$ as reference compound. The experimental data, presented in Figure 4, give $k(OH+CF_3CF_2CH_2OCH_3)/k(OH+CF_3CH_2OCH_3)$ = 1.158 ± 0.016 and $k(OH+CHF_2CF_2CH_2OCH_3)/k(OH+CF_3CH_2OCH_3)$ = 1.55 ± 0.07, Table 2. There are two studies of the OH reaction with $CF_3CH_2OCH_3$ giving rate coefficients of (6.24 ± 0.67) and (5.4 ± 0.3) × 10^{-13} cm^3 molecule^{-1} s^{-1} at 298 K for the OH reaction of $CF_3CH_2OCH_3$ (*17*, *18*), and taking the weighted average of these numbers, (5.54 ± 0.27) × 10^{-13} cm^3 molecule^{-1} s^{-1}, we derive the OH reaction rate coefficient at 298 K of $CF_3CF_2CH_2OCF_3$ and $CHF_2CF_2CH_2OCF_3$ to be (6.42 ± 0.33) and (8.6 ± 0.6) × 10^{-13} cm^3 molecule^{-1} s^{-1}, respectively. An additional set of experiments on the OH reaction with $CHF_2CF_2CH_2OCF_3$ was carried out using $CHCl_3$ as the reference compound. The data, presented in graphical form as Supporting Information, give $k(OH+CHF_2CF_2CH_2OCH_3)/k(OH+CHCl_3)$ = 9.8 ± 0.9, Table 2, from which we derive $k(OH+CHF_2CF_2CH_2OCH_3)$ = (9.8 ± 1.7) × 10^{-13} cm^3 molecule^{-1} s^{-1} and a weighted average of (8.7 ± 0.5) × 10^{-13} cm^3 molecule^{-1} s^{-1} for this reaction at 298 K.

TABLE 3. Relative Rate Coefficients and Derived Absolute Rate Coefficients for the Cl Atom Reaction with a Series of Fluorinated Ethers and Esters at 298 K

HFE	reference compound[a]	k_{rel}	k_{Cl}/cm^3 molecule^{-1} s^{-1}	method[b]
$(CF_3)_2CHOCH_3$	CH_3OH	0.151 ± 0.013	(8.3 ± 1.8) × 10^{-12}	RR-GC/MS
	CH_3CH_2OH	0.089 ± 0.008	(8.5 ± 1.9) × 10^{-12}	RR-GC/MS
$CF_3CH_2OCH_2CF_3$	$CHCl_3$	6.9 ± 0.5	(6.6 ± 2.0) × 10^{-13}	RR-GC/MS
	CH_2Cl_2	1.87 ± 0.06	(6.17 ± 3.1) × 10^{-13}	RR-GC/MS
			(4.4 ± 0.4) × 10^{-13}	VLPR (*3*)
			(7.1 ± 0.9) × 10^{-13}	FTIR (*4*)
$CF_3CF_2CH_2OCH_3$	CH_3CH_2OH	0.419 ± 0.022	(4.0 ± 0.8) × 10^{-11}	RR-GC/MS
$CHF_2CF_2CH_2OCH_3$	$CF_3CH_2OCH_3$	1.146 ± 0.008	(2.65 ± 0.17) × 10^{-11}	RR-GC/MS
CF_3CH_2OCHO	$CHCl_3$	0.651 ± 0.026	(6.3 ± 1.9) × 10^{-14}	RR-GC/MS
	CHF_2CH_2F	1.998 ± 0.032		RR-GC/MS
			<4 × 10^{-13}	RR−FTIR (*4*)
CHF_2CH_2F	$CHCl_3$	3.07 ± 0.04 [c]	(3.0 ± 0.9) × 10^{-14}	RR-GC/MS
			(3.2 ± 0.9) × 10^{-14}	RR-GC/MS (*18*)

[a] Reaction rate coefficients of reference compounds (/cm^3 molecule^{-1} s^{-1}): k (Cl+CH_3OH) = (5.5 ± 1.1) × 10^{-11} (*12*), k(Cl+CH_3CH_2OH) = (9.6 ± 1.9) × 10^{-11} (*12*), k(Cl+$CHCl_3$) = (9.6 ± 3.0) × 10^{-14} (*12*), k (Cl+CH_2Cl_2) = (3.3 ± 1.7) × 10^{-13} (*12*), k(Cl+$CH_3CH_2OCH_3$) = (2.31 ± 0.15) × 10^{-11} (*3*).[b] RR, relative rate; FTIR, fourier transform infrared spectroscopy; GC, gas chromatography; MS, mass spectrometry; VLPR, very low-pressure reactor technique. [c] Relative reaction rate coefficient derived from the study of CF_3CH_2OCHO vs $CHCl_3$ and CF_3CH_2OCHO vs CHF_2CH_2F.

The formic acid ester of 2,2,2-trifluoroethanol, CF_3CH_2-OCHO, was found as the major product in the oxidation of $CF_3CH_2OCH_2CF_3$ (*2*, *4*), see later. The OH reaction with CF_3-CH_2OCHO was studied using three different reference compounds $CHCl_3$, CH_2ClCH_2Cl, and CHF_2CH_2F. The results are included in Table 2, while the experimental data are presented in graphical form as Supporting Information. We obtained the relative rates k(OH+CF_3CH_2OCHO)/k(OH+$CHCl_3$) = 0.720 ± 0.026, k(OH+CF_3CH_2OCHO)/k(OH+CH_2ClCH_2Cl) = 0.415 ± 0.027, and k(OH+CF_3CH_2-OCHO)/k(OH+CHF_2CH_2F) = 4.8 ± 0.4. The recommended OH rate coefficients for reaction with CHF_2CH_2F and CH_2-$ClCH_2Cl$ are (1.70 ± 0.34) × 10^{-14} (*12*) and (2.5 ± 0.7) × 10^{-13} (*19*) cm^3 molecule^{-1} s^{-1} at 298 K, respectively. Hence we derive the absolute values of (7.2 ± 1.1) × 10^{-14}, (1.03 ± 0.32) × 10^{-13}, and (8.2 ± 1.8) × 10^{-14} cm^3 molecule^{-1} s^{-1} and a weighted average of k(OH+CF_3CH_2OCHO) = (7.7 ± 0.9) × 10^{-14} cm^3 molecule^{-1} s^{-1} for the rate coefficient at 298 K. Thus, the ester reacts slower by a factor of 2 than the ether from which it stems, see later.

The Cl reaction with $(CF_3)_2CHOCH_3$ was studied using CH_3OH and CH_3CH_2OH as reference compounds. Figure 5 shows the data from two independent experiments in the form of ln{[$(CF_3)_2CHOCH_3$]$_0$/[$(CF_3)_2CHOCH_3$]$_t$} vs ln{[CH_3-OH]$_0$/[CH_3OH]$_t$} from which the relative rate was found to be k_{rel} = 0.151 ± 0.013. The recommended Cl rate coefficient for reaction with CH_3OH is (5.5 ± 1.1) × 10^{-11} cm^3 molecule^{-1} s^{-1} at 298 K (*12*), which places the absolute rate coefficient of the Cl reaction with $(CF_3)_2CHOCH_3$ at (8.3 ± 1.8) × 10^{-12} cm^3 molecule^{-1} s^{-1}, Table 3. The experimental data from the relative rate study using CH_3CH_2OH as the reference compound is given in graphical form as Supporting Information. Three experiments were carried out giving k_{rel} = 0.089 ± 0.008. The latest JPL data evaluation (*12*) has recommended a rate coefficient of (9.6 ± 1.9) × 10^{-11} cm^3 molecule^{-1} s^{-1} for the reaction between Cl and CH_3CH_2OH at 298 K. On an absolute scale, the derived Cl reaction rate coefficient of $(CF_3)_2CHOCH_3$ is therefore (8.5 ± 1.9) × 10^{-12} cm^3 molecule^{-1} s^{-1}—the weighted average of our results being k(Cl+$(CF_3)_2$-$CHOCH_3$) = (8.4 ± 1.3) × 10^{-12} cm^3 molecule^{-1} s^{-1} at 298 K.

The study of the Cl atom reaction with $CF_3CH_2OCH_2CF_3$ was undertaken using CH_2Cl_2 and $CHCl_3$ as references resulting in the relative rates k(Cl+$CF_3CH_2OCH_2CF_3$)/k(Cl+CH_2Cl_2) = 1.87 ± 0.06 and k(Cl+$CF_3CH_2OCH_2CF_3$)/k(Cl+$CHCl_3$) = 6.9 ± 0.5. The results are included in Table 3, while the experimental data are presented in graphical form as Supporting Information. The recommended values for the reactions of CH_2Cl_2 and $CHCl_3$ with Cl atoms are (3.3 ± 1.7) × 10^{-13} and (9.6 ± 2.9) × 10^{-14} at 298 K (*12*), respectively, from which we derive absolute rates of (6.2 ± 3.1) and (6.6 ± 2.0) × 10^{-13} cm^3 molecule^{-1} s^{-1}. The weighted average of our results is k(Cl+$CF_3CH_2OCH_2CF_3$) = (6.5 ± 1.7) × 10^{-13} cm^3 molecule^{-1} s^{-1} at 298 K, which compares well, within the experimental uncertainties, with the results from a relative rate study of Wallington et al. (*4*), whereas the result from an absolute rate study by Kambanis et al. (*3*) using the very low-pressure reactor technique (VLPR) is about 30% lower, Table 3. The spread in the results may in part be attributed to the fact that CF_3 radicals are released during the oxidation of $CF_3CH_2OCH_2CF_3$ and that the subsequent reactions of CF_3O radicals are influencing the results.

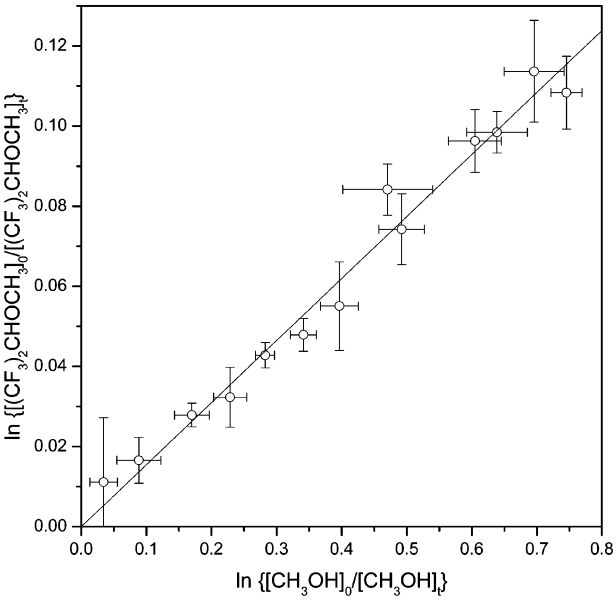

FIGURE 5. Decay of $(CF_3)_2CHOCH_3$ and CH_3OH in the presence of Cl atoms at 298 K plotted as ln{[$(CF_3)_2CHOCH_3$]$_0$/[[$(CF_3)_2CHOCH_3$]$_t$} vs ln{[CH_3OH]$_0$/[CH_3OH]$_t$}. Thirteen data points from 2 independent experiments were analyzed according to eq 2 giving a relative rate k_{rel} = 0.151 ± 0.013 (3σ error).

The Cl atom reaction rate with $CF_3CF_2CH_2OCH_3$ was measured relative to C_2H_5OH giving k(Cl+$CF_3CF_2CH_2OCH_3$)/k(Cl+C_2H_5OH) = (0.419 ± 0.022), Table 3. The experimental data are found in graphical form as Supporting Information. Taking k(Cl+C_2H_5OH) = (9.6 ± 1.9) × 10^{-11} cm^3 molecule^{-1} s^{-1} at 298 K (*12*) places k(Cl+$CF_3CF_2CH_2OCH_3$) = (4.0 ± 0.8) × 10^{-11} cm^3 molecule^{-1} s^{-1}. The $CHF_2CF_2CH_2OCH_3$ reaction

rate with Cl atoms was studied relative to $CF_3CH_2OCH_3$. The experimental data are given in graphical form as Supporting Information; the relative rate obtained is $k_{rel} = (1.146 \pm 0.008)$, Table 3. Taking $k(Cl+CF_3CH_2OCH_3) = (2.31 \pm 0.15) \times 10^{-11}$ cm^3 $molecule^{-1}$ s^{-1} at 298 K (*3*) places $k(Cl+CHF_2CF_2CH_2OCH_3) = (2.65 \pm 0.17) \times 10^{-11}$ cm^3 $molecule^{-1}$ s^{-1}. The relative magnitude of the rate coefficients for Cl-atoms with $CF_3CF_2CH_2OCH_3$ and $CHF_2CF_2CH_2OCH_3$ is not what would be expected—the compound with the most hydrogen should react the fastest. The absolute value of $k(Cl+C_2H_5OH)$ is well-determined (*12*), whereas only study reports $k(Cl+CHF_2CF_2CH_2OCH_3$ (*3*). In the same study is also reported a value for $k(Cl+CF_3CF_2OCH_2CF_3)$, which is ca. 30% lower than the results of Wallington et al. (*4*) as well as the present results, Table 3. We tentatively suggest that the error limit assigned to $k(Cl+CF_3CH_2OCH_3)$ (*3*) is too small and that the reactivities of $CF_3CF_2CH_2OCH_3$ and $CHF_2CF_2CH_2OCH_3$ toward Cl-atoms are identical within the experimental uncertainty.

The rate coefficient of the $CF_3CF_2CH_2OCHO$ reaction with Cl atoms was measured relative to $CHCl_3$ and CHF_2CH_2F. The results are included in Table 3, while the experimental data are given in graphical form as Supporting Information. The $CHCl_3$ experiments gave a relative rate $k(Cl+CF_3CF_2CH_2OCHO)/k(Cl+CHCl_3) = (0.651 \pm 0.026)$ from which an absolute rate coefficient for the Cl reaction with $CF_3CF_2CH_2OCHO$ of $(6.3 \pm 1.9) \times 10^{-14}$ cm^3 $molecule^{-1}s^{-1}$ at 298 K was derived. This is an order of magnitude slower than the estimated upper limit for this reaction given by Wallington et al. (*4*). The CHF_2CH_2F experiments gave a relative rate $k(Cl+CF_3CF_2CH_2OCHO)/k(Cl+CHF_2CH_2F) = (1.998 \pm 0.032)$. Taking $k(Cl+CHF_2CH_2F) = 4.9 \times 10^{-14}$ cm^3 $molecule^{-1}$ s^{-1} at 298 K (*12*) places $k(Cl+CF_3CF_2CH_2OCHO) = 9.8 \times 10^{-14}$ cm^3 $molecule^{-1}$ s^{-1} on an absolute scale, which is outside the error limit of the result obtained using $CHCl_3$ as reference compound.

CHF_2CH_2F is from a chemical point of view ideal as a reference compound in the present study of HFEs. Unfortunately, its reaction rate coefficient with Cl atoms is inadequately determined, and the assigned uncertainty factor in the latest JPL evaluation is 3 (*12*). On the other hand, we may derive $k(Cl+CHF_2CH_2F)$ indirectly from the two experiments and obtain $k(Cl+CHF_2CH_2F)/k(Cl+CHCl_3) = 3.07 \pm 0.04$, Table 3. Taking $k(Cl+CHCl_3) = (9.6 \pm 3.0) \times 10^{-14}$ cm^3 $molecule^{-1}$ s^{-1} places $k(Cl+CHF_2CH_2F)$ at $(3.0 \pm 0.9) \times 10^{-14}$ cm^3 $molecule^{-1}$ s^{-1} at 298 K in agreement with recent results of Oyaro et al. (*18*). Thus, the present data suggest the Cl reaction rate coefficient of CHF_2CH_2F to be 35% lower than that reported by Tschuikow-Roux et al. from relative rate studies (*20*).

There is a clear correlation (correlation coefficient ~0.8) between the logarithms of the OH and the Cl rate coefficients with the same substrate suggesting that the preferred site of reaction may be the same for the two radicals. In a recent study of 9 other HFEs we find a similar correlation coefficient of 0.93 (*18*). To be discussed below, this may in part be rationalized in terms of the quite different C−H bond dissociation enthalpies of the >CH-, $-CH_2-$, and $-CH_3$ groups in the hydrofluoroethers.

Atmospheric Fate of the HFEs. Hydrofluoroethers have a very slow rate of dissolution in water with their uptake coefficients ranging from 10^{-6} to 10^{-8} (*21*). Uptake in rainwater or cloud droplets is therefore not an important atmospheric sink for HFEs, and the major fate of the HFEs in the troposphere is reaction with OH. The same products were observed being formed during the OH and Cl reactions with the HFEs studied, and more detailed product studies were only carried out employing Cl atoms as the initiating oxidant.

The atmospheric fate of $CF_3CH_2OCH_2CF_3$ has previously been addressed by O'Sullivan et al. (*2*) and Wallington et al. (*4*). Both studies, based on FTIR detection, report the formate CF_3CH_2OCHO as the major product (≥96%) and the trifluoroacetate $CF_3CH_2OC(O)CF_3$ as a minor product in an atmosphere containing excess NO. In an atmosphere with only traces of NO present they observed ca. 15% yield of $CF_3CH_2OC(O)CF_3$, and Wallington et al. (*4*) concluded that the main route of the alkoxy radicals, $CF_3CH_2OCH(\dot{O})CF_3$, under atmospheric conditions is C−C bond scission (reaction 12a) to give the formate and a CF_3 radical and that abstraction of the α-H by O_2 (reaction 11) is of minor importance.

$$CF_3CH_2OCH_2CF_3 + Cl \rightarrow CF_3CH_2O\dot{C}HCF_3 + HCl \quad (6)$$

$$CF_3CH_2O\dot{C}HCF_3 + O_2 + M \rightarrow CF_3CH_2OCH(O\dot{O})CF_3 + M \quad (7)$$

$$CF_3CH_2OCH(O\dot{O})CF_3 + NO \rightarrow CF_3CH_2OCH(\dot{O})CF_3 + NO_2 \quad (8a)$$

$$\rightarrow CF_3CH_2OCH(ONO_2)CF_3 \quad (8b)$$

$$CF_3CH_2OCH(O\dot{O})CF_3 + HO_2 \rightarrow CF_3CH_2OCH(OOH)CF_3 + O_2 \quad (9a)$$

$$\rightarrow CF_3CH_2OC(O)CF_3 + H_2O + O_2 \quad (9b)$$

$$2CF_3CH_2OCH(O\dot{O})CF_3 \rightarrow 2CF_3CH_2OCH(\dot{O})CF_3 + O_2 \quad (10a)$$

$$\rightarrow CF_3CH_2OCH(OH)CF_3 + CF_3CH_2OC(O)CF_3 + O_2 \quad (10b)$$

$$CF_3CH_2OCH(\dot{O})CF_3 + O_2\ (\rightarrow)\ CF_3CH_2OC(O)CF_3 + HO_2 \quad (11)$$

$$CF_3CH_2OCH(\dot{O})CF_3 + M \rightarrow CF_3CH_2OCHO + \dot{C}F_3 + M \quad (12a)$$

$$\rightarrow CF_3CH_2\dot{O} + CF_3CHO + M \quad (12b)$$

During our study of $CF_3CH_2OCH_2CF_3$ we detected two primary oxidation products: (i) $CF_3CH_2OC(O)CF_3$ (m/z = 197, $[CF_3CH_2OC(O)CF_3]H^+$) and CF_3CH_2OCHO (m/z = 129, $[CF_3CH_2OC(O)H]H^+$). Figure 6 shows the PCI-MS signals of the ions m/z = 183, 197, and 129 of the parent HFE and the two oxidation products, extracted from complete PCI-MS chromatograms, as a function of photolysis time in a study carried out in an 'NO-free' atmosphere. Assuming that the MS response functions of CF_3CH_2OCHO and $CF_3CH_2OC(O)CF_3$ are identical the estimated yields of the two esters are 85 ± 5% CF_3CH_2OCHO and 15 ± 5% $CF_3CH_2OC(O)CF_3$, in agreement with the previous results for this reaction (*2*, *4*). As can be seen from Figure 6, the formate CF_3CH_2OCHO slowly undergoes further reaction ($k(Cl+CF_3CH_2OCHO) \sim 5 \times 10^{-14}$ cm^3 $molecule^{-1}s^{-1}$, this study), whereas the trifluoroacetyl ester, $CF_3CH_2OC(O)CF_3$, obviously is far less reactive ($k(Cl+CF_3CH_2OC(O)CF_3) \sim 9 \times 10^{-16}$ cm^3 $molecule^{-1}$ s^{-1}(*4*)). A similar experiment, but with 10 ppm NO added to the air, resulted in a 98 ± 2% yield of CF_3CH_2OCHO, again in agreement with the results of Wallington et al. (*4*).

In the oxidation of $(CF_3)_2CHOCH_3$ two primary products were identified with MS base ion signals m/z at 197 and 129. Figure 7 shows the intensities of the PCI-MS signals of selected, characteristic ions from the parent molecule and the two products, extracted from complete PCI-MS chromatograms, as a function of time in a Cl oxidation experiment without NO added to the reaction chamber. The major product (>99%) was identified as $CF_3C(O)OCH_3$ (m/z = 129, $[CF_3C(O)OCH_3]H^+$), while the minor product is $(CF_3)_2$-

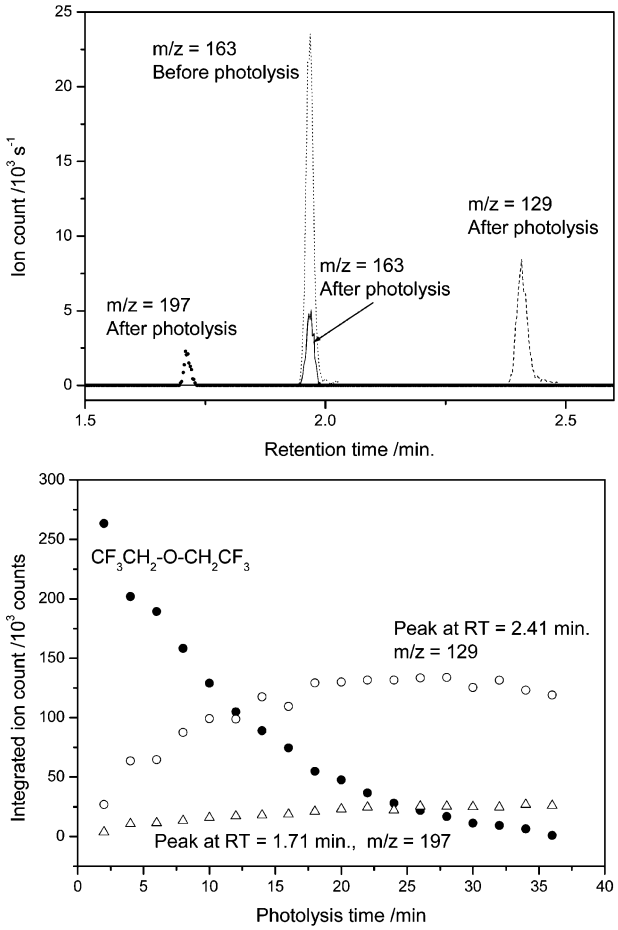

FIGURE 6. Top: GC-MS chromatogram (SIM) of a $CF_3CH_2OCH_2CF_3$/Cl_2 reaction mixture before photolysis and after 35 min of photolysis. Bottom: Integrated MS ion count of the three peaks in the gas-chromatogram as a function of time.

CHOCHO ($m/z = 197$, $[(CF_3)_2CHOCHO]H^+$). (Note that the PCI-MS signal for $m/z = 197$ has been expanded by a factor of 10 in Figure 7.) The major route of the reaction is thus H-abstraction from the tertiary carbon atom (reaction 13a), eventually followed by C−C bond scission to give methyl trifluoroacetate, $CF_3C(O)OCH_3$, and CF_3 radicals.

$$(CF_3)_2CHOCH_3 + Cl \rightarrow (CF_3)_2\dot{C}OCH_3 + HCl \quad (13a)$$

$$(\rightarrow)(CF_3)_2CHO\dot{C}H_2 + HCl \quad (13b)$$

$$(CF_3)_2\dot{C}OCH_3 + O_2 + M \rightarrow (CF_3)_2C(O\dot{O})OCH_3 + M \quad (14)$$

$$(CF_3)_2C(O\dot{O})OCH_3 + NO \rightarrow (CF_3)_2C(\dot{O})OCH_3 + NO_2 \quad (15a)$$

$$\rightarrow (CF_3)_2C(ONO_2)OCH_3 \quad (15b)$$

$$(CF_3)_2C(O\dot{O})OCH_3 + HO_2 \rightarrow (CF_3)_2C(OOH)OCH_3 + O_2 \quad (16)$$

$$2(CF_3)_2C(O\dot{O})OCH_3 \rightarrow 2(CF_3)_2C(\dot{O})OCH_3 + O_2 \quad (17)$$

$$(CF_3)_2C(\dot{O})OCH_3 + M \rightarrow CF_3C(O)OCH_3 + \dot{C}F_3 + M \quad (18)$$

Two products were detected during the degradation of $CF_3CF_2CH_2OCH_3$, both with m/z of 179. Figure 8 shows the intensities of the PCI-MS signals of selected, characteristic ions from the parent molecule and the two products, extracted from complete PCI-MS chromatograms, as a function of time in a Cl oxidation experiment without NO added to the reaction chamber. The minor product (<5%) was identified by its retention time as the formate CF_3CF_2-CH_2OCHO ($m/z = 179$, $[CF_3CF_2CH_2OCHO]H^+$), while the major product is the methyl perfluoropropanate CF_3CF_2C-$(O)OCH_3$ ($m/z = 197$, $[CF_3CF_2C(O)CH_3]H^+$). The major route in the initial oxidation of $CF_3CF_2CH_2OCH_3$ is therefore H-abstraction from the methylene group (reaction 19a).

$$CF_3CF_2CH_2OCH_3 + Cl \rightarrow CF_3CF_2\dot{C}HOCH_3 + HCl \quad (19a)$$

$$(\rightarrow)\ CF_3CF_2CH_2O\dot{C}H_2 + HCl \quad (19b)$$

$$CF_3CF_2\dot{C}HOCH_3 + O_2 + M \rightarrow CF_3CF_2CH(O\dot{O})OCH_3 + M \quad (20)$$

$$CF_3CF_2CH(O\dot{O})OCH_3 + NO \rightarrow CF_3CF_2CH(\dot{O})OCH_3 + NO_2 \quad (21a)$$

$$\rightarrow CF_3CF_2CH(ONO_2)OCH_3 \quad (21b)$$

$$CF_3CF_2CH(O\dot{O})OCH_3 + HO_2 \rightarrow CF_3CF_2CH(OOH)OCH_3 + O_2 \quad (22a)$$

$$\rightarrow CF_3CF_2CH(\dot{O})OCH_3 + H_2O + O_2 \quad (22b)$$

$$2CF_3CF_2CH(O\dot{O})OCH_3 \rightarrow 2CF_3CF_2CH(\dot{O})OCH_3 + O_2 \quad (23a)$$

$$\rightarrow CF_3CF_2CH(OH)OCH_3 + CF_3CF_2C(O)OCH_3 + O_2 \quad (23b)$$

$$CF_3CF_2CH(\dot{O})OCH_3 + O_2 \rightarrow CF_3CF_2CH(O)OCH_3 + HO_2 \quad (24)$$

$$CF_3CF_2CH(\dot{O})OCH_3 + M\ (\rightarrow) CF_3\dot{C}F_2 + CH(O)OCH_3 + M \quad (25)$$

We did not observe the formation of methylformate, CH_3-$OCHO$ (reaction 25), suggesting that C−C bond scission in the alkoxy radical to give the CF_3CF_2 radical is not an important route in the degradation.

The oxidative degradation of $CHF_2CF_2CH_2OCH_3$ follows closely that of $CF_3CF_2CH_2OCH_3$ given above. Again, two products were identified namely $CHF_2CF_2CH_2OCHO$ with $m/z = 161$, $[CHF_2CF_2CH_2OCHO]H^+$, and $CHF_2CF_2C(O)OCH_3$ also with $m/z = 161$, $[CHF_2CF_2C(O)OCH_3]H^+$. Figure 9 shows the intensities of the PCI-MS signals of selected ions from the parent molecule and the two products, extracted from complete PCI-MS chromatograms, as a function of time in a Cl oxidation experiment without NO added to the reaction chamber. Based on the retention times, the main product (> 90%) is suggested to be $CHF_2CF_2C(O)OCH_3$.

In summary, the atmospheric degradation products of the HFEs studied are esters:

$$(CF_3)_2CHOCH_3 \xrightarrow{Ox} CF_3C(O)OCH_3$$

$$CF_3CH_2OCH_2CF_3 \xrightarrow{Ox} CF_3CH_2OCHO$$

$$CF_3CF_2CH_2OCH_3 \xrightarrow{Ox} CF_3CF_2C(O)OCH_3$$

$$CHF_2CF_2CH_2OCH_3 \xrightarrow{Ox} CHF_2CF_2C(O)OCH_3$$

The preferred site of reaction may in part be rationalized in terms of the C−H bond dissociation enthalpies (BDE_{C-H}), for which an empirical interpolation/estimation method based on DFT calculations recently has been presented (*22*). The method predicts rather large differences in the C−H

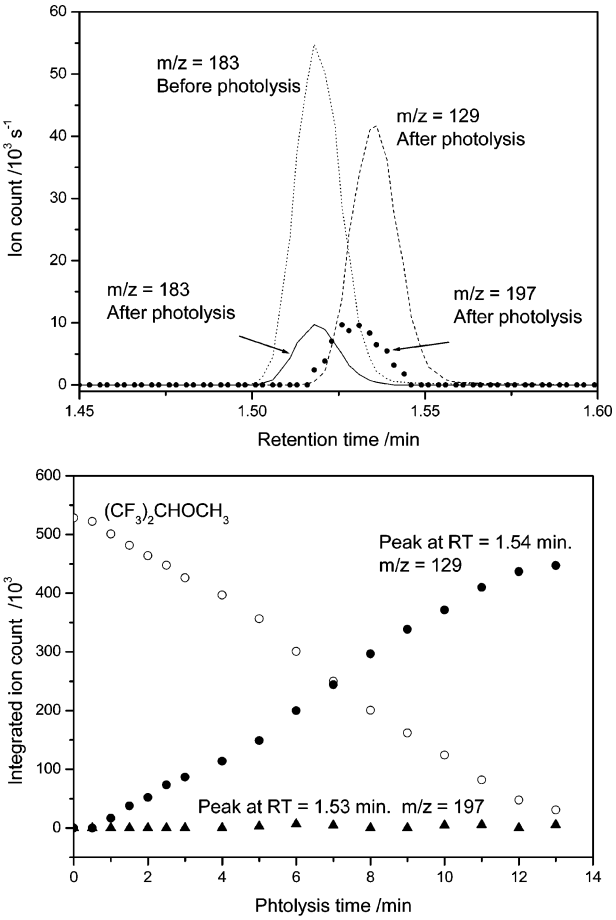

FIGURE 7. Top: GC-MS chromatogram (SIM) of a $(CF_3)_2CHOCH_3/Cl_2$ reaction mixture before photolysis and after 13 min of photolysis. Bottom: Integrated ion count of the three peaks in the gas-chromatogram as a function of time.

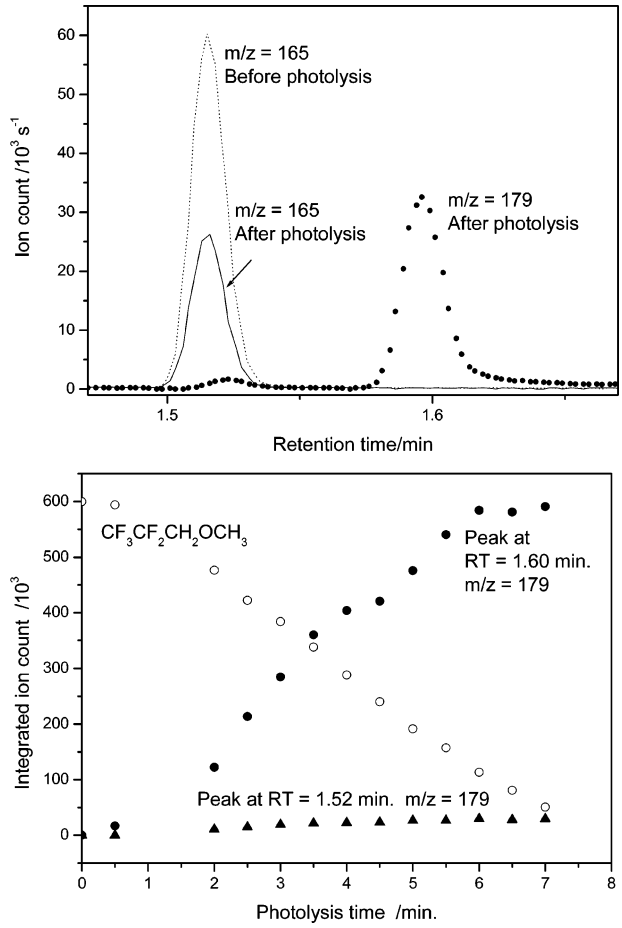

FIGURE 8. Top: GC-MS chromatogram (SIM) of a $CF_3CF_2CH_2OCH_3/Cl_2$ reaction mixture before photolysis and after 4 min of photolysis. Bottom: Integrated ion count of the three peaks in the gas-chromatogram as a function of time.

bond dissociation enthalpies: $BDE_{C-H}(CF_3CF_2C\mathbf{H}_2OCH_3) \approx 396$, $BDE_{C-H}((CF_3)_2C\mathbf{H}OCH_3) \approx 397$, $BDE_{C-H}(CF_3C\mathbf{H}_2OC\mathbf{H}_2CF_3) \approx 405$, $BDE_{C-H}(CF_3CF_2CH_2OC\mathbf{H}_3) \approx BDE_{C-H}(CHF_2CF_2CH_2OC\mathbf{H}_3) \approx 406$, $BDE_{C-H}((CF_3)_2CHOC\mathbf{H}_3) \approx 416$, and $BDE_{C-H}(C\mathbf{H}F_2CF_2CH_2OCH_3) \approx 425$ kJ mol^{-1}. In fact, the differences are so large that only one major site of the initial radical attack is expected in each of the HFE studied. The esters originating from the HFEs are apparently all less reactive toward gas-phase oxidants than their parent HFEs. They may likely dissolve in droplets and aerosols, hydrolyze, and undergo further oxidation in the liquid phase. That is, the HFEs studied may end up as fluorinated acids in the environment.

Atmospheric Lifetimes and Global Warming Potentials. The atmospheric lifetimes of $(CF_3)_2CHOCH_3$, $CF_3CH_2OCH_2CF_3$. $CF_3CF_2CH_2OCH_3$, and $CHF_2CF_2CH_2OCH_3$ due to removal by reaction with OH radicals, τ_{OH}, may be estimated from the data obtained in this study. Using the determined OH rate coefficients, a global averaged concentration of OH radicals equal to 9.4×10^5 radicals cm^{-3} (*23*), the following lifetimes of $(CF_3)_2CHOCH_3$, $CF_3CH_2OCH_2CF_3$, $CF_3CF_2CH_2OCH_3$, and $CHF_2CF_2CH_2OCH_3$ in the gas-phase are found: $\tau_{OH}((CF_3)_2CHOCH_3) \sim 100$ days; $\tau_{OH}(CF_3CH_2OCH_2CF_3) > 80$ days; $\tau_{OH}(CF_3CF_2CH_2OCH_3) \sim 18$ days; $\tau_{OH}(CHF_2CF_2CH_2OCH_3) \sim 14$ days. The atmospheric lifetime of the HFE oxidation product, CF_3CH_2OCHO, due to removal by reaction with OH radicals is estimated to be $\tau_{OH}(CF_3CH_2OCHO) > 160$ days.

Pinnock et al. (*24*) have provided a simple method for estimating the instantaneous cloudy-sky radiative forcing (*IF*) directly from a molecule's absorption cross-sections. Global warming potentials, $GWP(t)$, for CF_3CHO and CF_3CH_2CHO, relative to CFC-11, can then be calculated from the following expression (*25*):

$$GWP(t) = \frac{IF_{ald}}{IF_{CFC-11}} \frac{\tau_{ald}}{\tau_{CFC-11}} \frac{M_{ald}}{M_{CFC-11}} \left(\frac{1 - \exp(-t/\tau_{ald})}{1 - \exp(-t/\tau_{CFC-11})} \right) \quad (26)$$

where M is the molecular mass and t is the time horizon over which the instantaneous forcing is integrated. Instantaneous forcings and global warming potentials for a 20- and 100-year time horizon for $(CF_3)_2CHOCH_3$, $CF_3CH_2OCH_2CF_3$, $CF_3CF_2CH_2OCH_3$, and $CHF_2CF_2CH_2OCH_3$ are collected in Table 4. The data on CFC-11 were taken from the work of Pinnock and co-workers (*24*). Although the instantaneous forcings of the HFEs are relatively large compared to that of CFC-11, their global warming potentials are moderate due to their relatively short lifetimes.

Care must be exercised when applying these results. These calculations are based on the assumption that the HFEs are evenly distributed over the whole globe. This is an approximation since their atmospheric lifetimes are relatively short. Further, the instantaneous forcings are based on a 1 ppbv increase in their atmospheric concentrations. One may question how realistic this release scenario is; to provide realistic predictions, advanced three-dimensional chemical tracer modeling and radiative forcing calculations are needed. However, we justify the calculations because they provide a reasonable estimate of the atmospheric lifetimes and global warming potentials of the HFEs. This information is im-

TABLE 4. Estimated Global Warming Potentials, *GWP*(*t*), of Four C_4-Hydrofluoroethers for 20- and 100-Year Time Horizons, Relative to CFC-11[b]

compound	k_{OH}/cm^3 molecule^{-1} s^{-1}	τ_{OH}/y	IF/W m^{-2}	GWP(20)	GWP(100)
$(CF_3)_2CHOCH_3$	1.27×10^{-13}	0.266	0.309	0.0145	0.00565
$CF_3CH_2OCH_2CF_3$	1.51×10^{-13}	0.223	0.334	0.0132	0.0050
$CF_3CF_2CH_2OCH_3$	6.42×10^{-13}	0.053	0.276	0.0028	0.0011
$CHF_2CF_2CH_2OCH_3$	8.7×10^{-13}	0.039	0.237	0.0020	0.0008
CFC-11		50.00[a]	0.26[a]	1.0000	1.0000

[a] From the IPCC report 2001 (*26*). [b] The instantaneous cloudy-sky radiative forcings, *IF*, for a 1 ppbV increase in atmospheric concentrations were calculated according to the procedure given by Pinnock et al. (*24*). The atmospheric lifetimes, τ_{OH}, were calculated from a global average OH concentration of 9.4×10^5 radicals cm^{-3} (*23*).

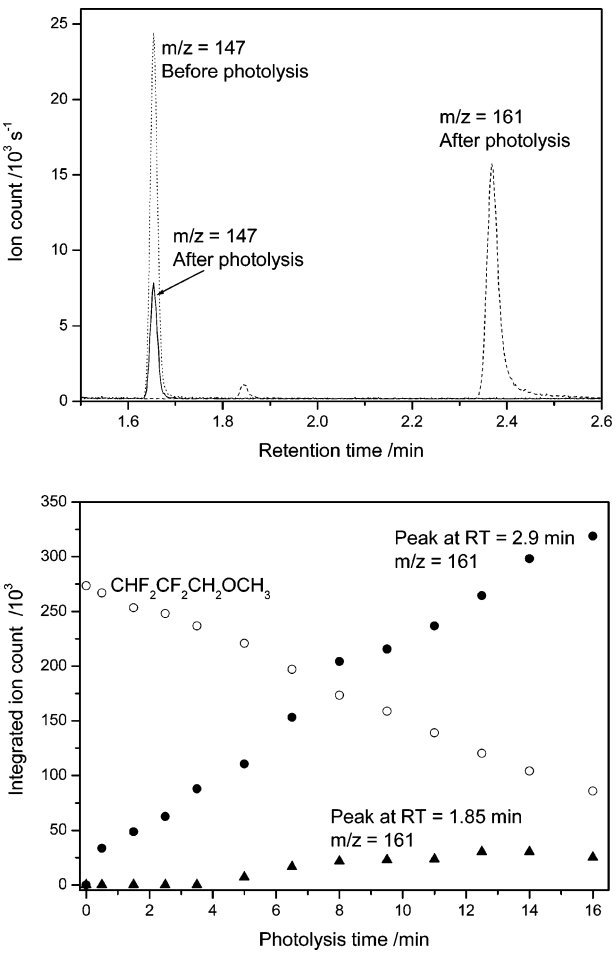

FIGURE 9. Top: GC-MS chromatogram (SIM) of a $CHF_2CF_2CH_2OCH_3$/Cl_2 reaction mixture before photolysis and after 16 min of photolysis. Bottom: Integrated MS ion count of the three peaks in the gas-chromatogram as a function of time.

portant when assessing the total environmental burden of possible HCFC/HFC replacement compounds. Pinnock et al. (*24*) has reported that the model generally overestimates the real forcing by as much as 29% when calculating the instantaneous radiative forcing directly from the absorption cross-sections. It is therefore likely that the present results provide upper estimates for the global warming potentials. The conclusion, however, is unaltered: the HFEs studied have very low global warming potentials.

Acknowledgments

This work is part of the project "Impact of Fluorinated Alcohols and Ethers on the Environment" (IAFAEE) and has received support from the CEC Environment and Climate program through contract ENVK2-1999-00099. We would like to thank Dr. Earle Waghorne, University College Dublin, Ireland, for making his results from uptake measurements of hydrofluorinated ethers available to us prior to publication. N.O. acknowledges a scholarship under the Norwegian Quota Program.

Supporting Information Available

PCI-MS spectra of the compounds used in the study and additional kinetic data for OH radical and Cl atom reactions with the compounds studied. This material is available free of charge via the Internet at http://pubs.acs.org.

Literature Cited

(1) Orkin, V. L.; Villenave, E.; Huie, R. E.; Kurylo, M. J. *J. Phys. Chem., A* **1999**, *103*, 9770−9779.
(2) O'Sullivan, N.; Wenger, J.; Sidebottom, H.; Treacy, J. In *The oxidizing capacity of the troposphere. Proceedings of the Seventh European Commission Symposium on physicochemical behaviour of atmospheric pollutants*; Larsen, B., Versino, B., Eds.: Venice, Italy, 1997; pp 77−79.
(3) Kambanis, K. G.; Lazarou, Y. G.; Papagiannakopoulos, P. *J. Phys. Chem., A* **1998**, *102*, 8620−8625.
(4) Wallington, T. J.; Guschin, A.; Stein, T. N. N.; Platz, J.; Sehested, J.; Christensen, L. K.; Nielsen, O. J. *J. Phys. Chem., A* **1998**, *102*, 1152−1161.
(5) Sihra, K.; Hurley, M. D.; Shine, K. P.; Wallington, T. J. *J. Geophys. Res. [Atmos.]* **2001**, *106*, 20493−20505.
(6) York, D. *Can. J. Phys.* **1966**, *44*, 1079−1086.
(7) Huang, Y.; Gu, Y.; Liu, C.; Yang, X.; Tao, Y. *Chem. Phys. Lett.* **1986**, *127*, 432−437.
(8) Aker, P. M.; Sloan, J. J. *J. Chem. Phys.* **1986**, *85*, 1412−1417.
(9) Streit, G. E.; Whitten, G. Z.; Johnston, H. S. *Geophys. Res. Lett.* **1976**, *3*, 521−523.
(10) Bailey, A. E.; Heard, D. E.; Paul, P. H.; Pilling, M. J. *J. Chem. Soc., Faraday Trans.* **1997**, *93*, 2915−2920.
(11) Ballard, J.; Knight, R. J.; Newnham, D. A.; Vander Auwera, J.; Herman, M.; Di Lonardo, G.; Masciarelli, G.; Nicolaisen, F. M.; Beukes, J. A.; Christensen, L. K.; McPheat, R.; Duxbury, G.; Freckleton, R.; Shine, K. P. *J. Quant. Spectrosc. Radiat. Transfer* **2000**, *66*, 109−128.
(12) Sander, S. P.; Friedl, R. R.; Golden, D. M.; Kurylo, M. J.; Huie, R. E.; Orkin, V. L.; Moortgat, G. K.; Ravishankara, A. R.; Kolb, C. E.; Molina, M. J.; Finlayson-Pitts, B. J. *Chemical Kinetics and Photochemical Data for Use in Atmospheric Studies. Evaluation Number 14*; National Aeronautics and Space Administration, Jet Propulsion Laboratory, California Institute of Technology: Pasadena, California, 2003.
(13) Oyaro, N.; Nielsen, C. J. *Asian Chem. Lett.* **2003**, *7*, 119−122.
(14) Wallington, T. J.; Ball, J. C. *J. Phys. Chem.* **1995**, *99*, 3201−3205.
(15) Sehested, J.; Wallington, T. J. *Environ. Sci. Technol.* **1993**, *27*, 146−152.
(16) Sellevåg, S. R.; Kelly, T.; Sidebottom, H.; Nielsen, C. J. *Phys. Chem. Chem. Phys.* **2004**, *6*, 1243−1252.
(17) Zhang, Z.; Saini, R. D.; Kurylo, M. J.; Huie, R. E. *J. Phys. Chem.* **1992**, *96*, 9301−9304.
(18) Oyaro, N.; Sellevåg, S. R.; Nielsen, C. J. *J. Phys. Chem.* **2004**, Submitted.
(19) Atkinson, R. *J. Phys. Chem. Ref. Data, Monograph* **1994**, *2*, 1−216.
(20) Tschuikow-Roux, E.; Yano, T.; Niedzielski, J. *J. Chem. Phys.* **1985**, *82*, 65−74.
(21) Waghorne, E., personal communication.
(22) Urata, S.; Takada, A.; Uchimaru, T.; Chandra, A. K.; Sekiya, A. *J. Fluor. Chem.* **2002**, *116*, 163−171.
(23) Prinn, R. G.; Huang, J.; Weiss, R. F.; Cunnold, D. M.; Fraser, P. J.; Simmonds, P. G.; McCulloch, A.; Harth, C.; Salameh, P.;

O'Doherty, S.; Wang, R. H. J.; Porter, L.; Miller, B. R. *Science (Washington, DC, U.S.)* **2001**, *292*, 1882−1887.
(24) Pinnock, S.; Hurley, M. D.; Shine, K. P.; Wallington, T. J.; Smyth, T. J. *J. Geophys. Res. [Atmos.]* **1995**, *100*, 23227−23238.
(25) *Climate Change 1994: Radiative Forcing of Climate Change and An Evaluation of the IPCC IS92 Emission Scenarios*; Houghton, J. T., Meira Filho, L. G., Bruce, J., Lee, H., Callander, B. A., Haites, E., Harris, N., Maskell, K., Eds.; Intergovernmental Panel on Climate Change, Cambridge University Press: Cambridge, 1995.
(26) IPCC *Intergovernmental Panel on Climate Change (IPCC), 2001. Climate Change 2001: The Scientific Basis*; Cambridge University Press: Cambridge, U.K. and New York, U.S.A., 2001.

Received for review February 19, 2004. Revised manuscript received July 27, 2004. Accepted August 12, 2004.

ES0497330